CHAPTER 5

5. ANTIMICROBIAL ACTIVITY OF MARINE ACTINOMYCETES MEDIATED BIOSYNTHESIS OF SILVER NANOPARTICLES

5.1 INTRODUCTION

Nanotechnology deals with the synthesis and stabilization of various nanoparticles by physical and chemical processes. Currently, there is a growing need to develop an eco-friently process for nanoparticles synthesis. The word “nano” is used to indicate one billionth of a meter or 10^{-9}. Different types of nanomaterials like copper, zinc, titanium (Retchkiman-Schabes *et al.*, 2006), magnesium, gold (Gu *et al.*, 2003) and alginate (Ahmad *et al.*, 2005) have come up but silver nanoparticles have been proved to be most effective as it has good antimicrobial efficacy against bacteria, viruses and other eukaryotic micro-organisms (Gong *et al*., 2007).

The current investigation supports that use of silver ion or metallic silver as well as silver nanoparticles can be exploited in medicine for burn treatment, dental materials, coating stainless steel materials, textile fabrics, water treatment, sunscreen lotions, etc. and posses low toxicity to human cells, high thermal stability and low volatility (Duran *et al.*, 2007).

The silver nanoparticles show efficient antimicrobial property due to their extremely large surface area, which provides better contact with microorganisms. The nanoparticles get attached to the cell membrane and also penetrate inside the bacteria. The bacterial membrane contains sulfur-containing proteins and the silver nanoparticles interact with these proteins in the cell as well as with the phosphorus containing compounds like DNA. When silver nanoparticles enter into the bacterial cell it forms a low molecular weight region in the center of the bacteria to which the bacteria conglomerates thus, protecting the DNA from the silver ions. The nanoparticles preferably attack the respiratory chain, cell division finally leading to cell death. The nanoparticles releases silver ions in the bacterial cells, which enhancing their bactericidal

activity (Feng *et al.,* 2000; Sondi and Salopek-Sondi, 2007; Morones *et al.,* 2005; Song *et al.,* 2006).

The nanoparticles smaller than 10 nm interact with bacteria and produce electronic effects, which improve the reactivity of nanoparticles. Thus, it is corroborated that the bactericidal effect of silver nanoparticles are size reliant (Raimondi *et al.,* 2005; Morones *et al.,* 2005).

Silver nanoparticles are used for coating surgical masks (Li *et al.,* 2006), water filtration (Jain and Pradeep, 2005) and antimicrobial nanopaint can be developed (Kumar *et al.,* 2008).The nanocrystalline silver are used for dressings, creams, gel effectively reduce bacterial infections in chronic wounds (Richard *et al.,* 2002; Leaper, 2006; Ip *et al.,*2006).The silver nanoparticle containing polyvinyl nano-fibres which shows the efficient antibacterial property as wound dressing (Jun *et al.,* 2007).

Synthesis of nanoparticles using biological entities has great interest due to their unusual optical (Krolikowska *et al.,* 2003), chemical (Kumar *et al.,* 2003), photoelectrochemical (Chandrasekharan and Kamat, 2000) and electronic properties (Peto *et al.,* 2002). A wide variety of physical, chemical and biological processes results in the synthesis of nanoparticles, some of these are novel and others are quite common. For example, *Fusarium oxysporum* fungal biomass when exposed to aqueous $AgNO_3$ solution resulted in the extracellular formation of silver nanoparticles (Senapati *et al.,* 2004).

Nikhil *et al.* (2009) reported that the *Penicillium brevicompactum* WA 2315 fungus, utilized for compactin production and synthesis of nanomaterials. Supernatant was used for the biosynthesis of silver nanoparticles. The aqueous silver ions were reduced to silver nanoparticles when treated with the fungal supernatant. After 72h of treatment, silver nanoparticles obtained were in the range of 23–105 nm. It has been observed that, the extremophilic actinomycete, *Thermomonospora* sp. when exposed to

gold ions reduced the metal ions extracellularly, yielding gold nanoparticles with a much improved polydispersity (Sastry *et al.*, 2003).

Silver nanoparticles were synthesized by secondary metabolites producing *S.hygroscopicus*. UV-Visible absorbonce spectral analysis confirmed that the surface plasmon resonance of biosynthesis of AgNPs. EDXA and XRD are additional evidence of AgNPs and the crystalline nature of the synthesized AgNPs. (Sathya Sadhasivam *et al*., 2010).

The present study, made an attempt for the biosynthesis of silver nanoparticles using the marine actinomycetes. Marine actinomycetes are producing secondary metabolites culture supernatant inhibited different human pathogens, that supernatant have used for biosynthesis of silver nanoparticles. This approach gave silver nanoparticles as a co product that is useful as the metabolites for which the culture was utilized. It is industrially useful, feasible and commercially possible. To the best of our knowledge, this actinomycetes strain has been used for nanoparticles biosynthesis for first of its kind.

5.2 MATERIALS AND METHODS

5.2.1 Synthesis of silver nanoparticles by using selected actinomycetes

Representative of actinomycetes strains (+18, +50, and +118) were freshly inoculated in to ISP2 broth (Hi media) and incubated for five days on shaker at 120rpm at room temperature. The culture was centrifuged at 12,000 rpm for 5 minutes, and the supernatant was used for synthesis of silver nanoparticles (Bhainsa and Souza, 2006). Milli Q water was used for the synthesis of AgNPs. The supernatants was added separately to the reaction vessel containing silver nitrate at a concentration of 10^{-3} M the reaction between this supernatant and Ag^{+} ions was carried out. The mixture was allowed standing for different time interval (24, 48 and 72 hours).

5.2.2 Characterization of silver nanoparticles

Preliminary identification of the silver nanoparticles was carried out using UV-visible spectroscopy. Noble metals, especially gold (Au) and silver (Ag) nanoparticles exhibit unique and tunable optical properties on account of their surface plasmon resonance (SPR) dependent on the shape, size and size distribution of the nanoparticles (Mulvancy., 1996). The reduction of the Ag+ ions was monitored by measuring the UV-visible spectra of the solutions after diluting a small aliquot of the sample 20 times. UV-visible spectra were recorded on Hitachi double beam spectrophotometer (model U-2800) from 200-600 nm.

5.2.3 Purification of silver nanoparticles

The dry powder of the silver nanoparticles were obtained in the following manner: after desired reaction period, the (culture supernatant and silver nitrate) broth containing silver nanoparticles was centrifuged at 10,000 rpm for 15min, following which the pellet was re-dispersed in sterile distilled water get rid of any uncoordinated biological molecules. The process of centrifugation and re-dispersion in sterile double

distilled water was repeated thrice to ensure better separation of free entitles from the metal nanoparticles. The purified pellets were freeze dried using a lyophilizer (Tripathy *et al.,* 2009).

5.2.4 Analysis by Scanning Electron Microscopy (SEM)

After diluting the samples, it was directly placed a drop on the aluminum stub and allowed to dry and put under SEM microscope (Vigneshwaran *et al.,* 2007).

5.2.5 Analysis of X-Ray Diffraction (XRD)

The actinomycetes supernatant embedded with the silver nanoparticles was freeze-dried, powdered and used for XRD analysis. The diffracted intensities were recorded from 30-80 2θ angles (Vigneshwaran *et al.,* 2007).

5.2.6 Analysis of Fourier Transform Infrared Spectroscopy (FTIR)

In order to determine the functional groups on the cell surface that may be involved in the nanoparticle synthesis, FTIR spectrum was carried out. The tested sample were completely dried and blended with KBr to obtain a pellet. The FTIR spectra were collected at resolution of 4 cm^{-1} in the transmission mode (4000-400 cm^{-1}) using a perkin-Elmer FTIR spectrum (Pimprikar *et al.,* 2009).

5.2.7 Determination of antimicrobial activity by Paper disc methods

The AgNPs synthesized by using actinomycetes strains +18,+50 and +118 were tested for antimicrobial activity by disc diffusion assay against human pathogenic organisms such as *Staphylococcus aureus* gram positive and *E.coli* gram negative. The pure cultures of organisms were sub cultured on Muller- Hinton broth at 35^0C on a rotary shaker at 200rpm. Sterile wattman No: 1 paper cut 6mm diameter disc. Each strain was swabbed uniformly onto the plate using sterile cotton swab. Using a micropipette, 2µl of

the sample of nanoparticle solution was poured onto 6mm paper disc and put in center of all plates and incubated for 24 hours at 35^0C. The zone of inhibition was measured (Amanulla Mohammed Fayaz *et al*., 2010).

5.3 RESULTS

The present study was carred out antibacterial activity of extracellular biosynthesis of silver nanoparticles by using culture supernatant of actinomycetes (+18, +50, and +118 strains). Those cultures were inhibited different human pathogens in primary screening. In the secondary screening methods the culture supernatant showed inhibition against different human pathogens. Among the 3 strains used for the synthesis of silver nanoparticles, all the three strains (+18, +50, and +118) showed silver nanoparticles synthesis which was conformed by visual observation through the changes of colour from white to brown. However, no color change can be observed in the culture supernatant which was not found silver nanoparticles (Plate13, 14 & 15). The appearance of a dark red color in silver nitrate treated flask suggested the formation of silver nanoparticles. The silver nanoparticles were synthesized extracellularly. The nanoparticles were primarily characterized by UV–Visible spectroscopy, which has proved to be a very useful technique for the analysis of nanoparticles. In UV–Visible spectrum a strong, broad peak, located at 420 nm, was observed for silver nanoparticles prepared using the culture supernatant of +18, +50 and +118 (Fig. 3.1, 3.2 and 3.3). Observation of these peaks, assigned to a surface plasmon, was well documented for various metal nanoparticles with sizes ranging from 2 nm to 100 nm. A SEM micrograph on the nanoparticles present in the dry biomass was found their morphology (Plate 16, 17 & 18).

Further studies were carried out using X ray diffraction to confirm the crystalline nature of the particles, and the XRD pattern obtained was shown in (Figs. 3.4 - 3.6). The XRD pattern showed that, the intense peaks in the whole spectrum of 2θ values ranging from 10 to 100. It is important to know that, the exact nature of the silver particles formed and this can be deduced from the XRD spectrum of the sample. XRD spectra of pure crystalline silver structures have been published by the Joint Committee on Powder Diffraction Standards (JCPEF file no. 411402, (+18) 893722 (+50) and 87.0598 (+118)). A comparison of our XRD spectrum confirmed with the standard and the results showed that silver particles obtained in our experiments were in the form of nanocrystals as

evidenced by the peaks recored at 2θ values of such peaks, corresponding to 103, 111, 200, 100, 006 and 106 planes for silver respectively (Table 5.1). Moreover, such small insignificant impurity peaks are observed which may be attributed to other organic substances in culture supernatant. The Full Width at Half Maximum (FWHM) values measured for 111, 200 and 220 planes of reflection were used with the Debye–Scherrer equation to calculate the size of the nanoparticles. The particle sizes obtained using XRD.

The silver nanoparticle solution was extremely stable for nearly 65 days with only a little aggregation of particles. It has been reported that, the proteins can provide a good protecting environment for metal hydrosol during their growth processes. FTIR spectroscopy measurements are carried out to identify the biomolecules that bound specifically on the silver surface (Figs. 3.7, 3.8, 3.9 & Table 5.2).

The antimicrobial activity of AgNPs was investigated against gram positive and gram negative pathogenic organisms such as *Staphylococcus aureus* and *E.coli* using disc diffusion methods. Each well resulted that 2µl concentration of silver nanoparticles were showed appreciable inhibition and the results were given in Table 5.3.

Among the three strains (+18, +50 and +118) tested against two pathogens namely *E.coli* and *S.aureus*. The strain +18 showed high inhibition against *S.aureus* with 9 mm. whereas the *E.coli* growth was inhibited at 5 mm level. Similarly +50 and +118 strains showed higher inhibition against *S.aureus* with 8 mm each. Whereas the *E.coli* have the inhibition level of 7 and 6 mm with +50 and +118 strains respectively.

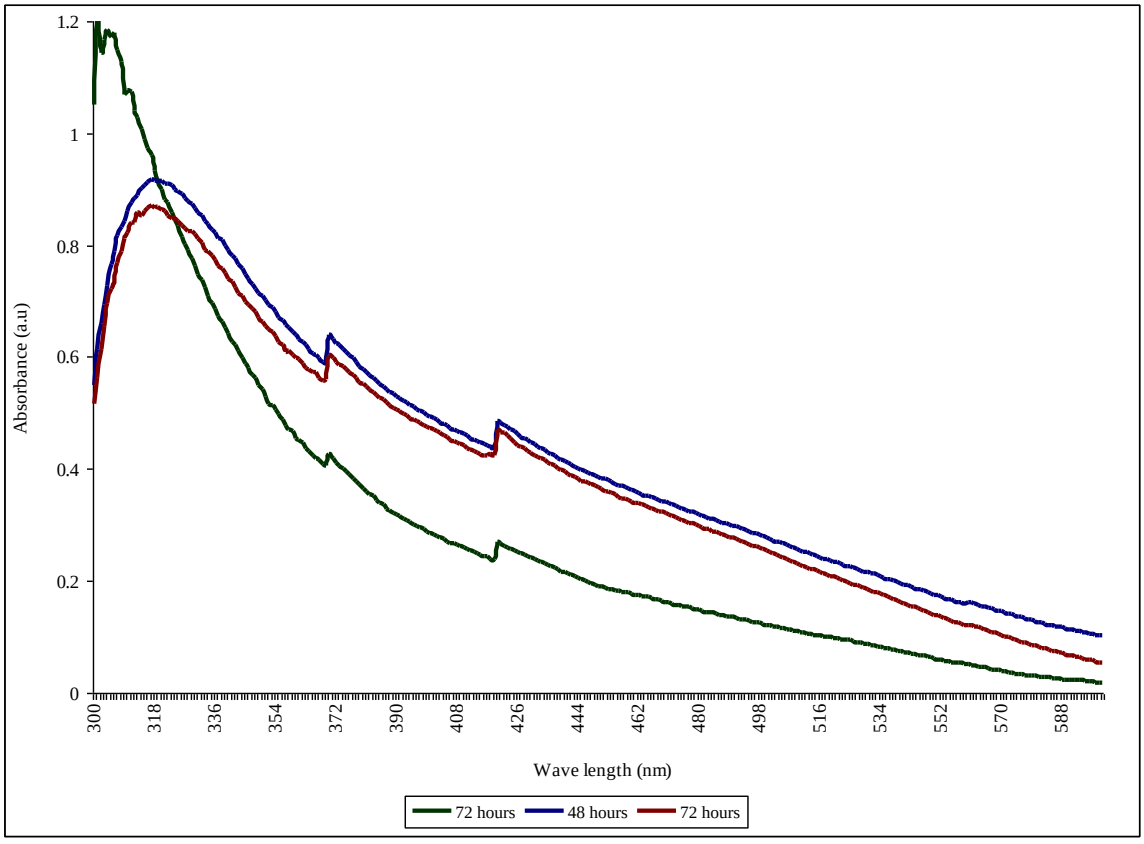

Fig. 3.1 UV- Visible spectra of actinomycete supernatant (+18) filtrate as a function of time at different incubations with silver nitrate (1mM) after 24h, 48h and 72h. respectively. The peak 420nm corresponds to the plasmon resonance of silver nanoparticles.

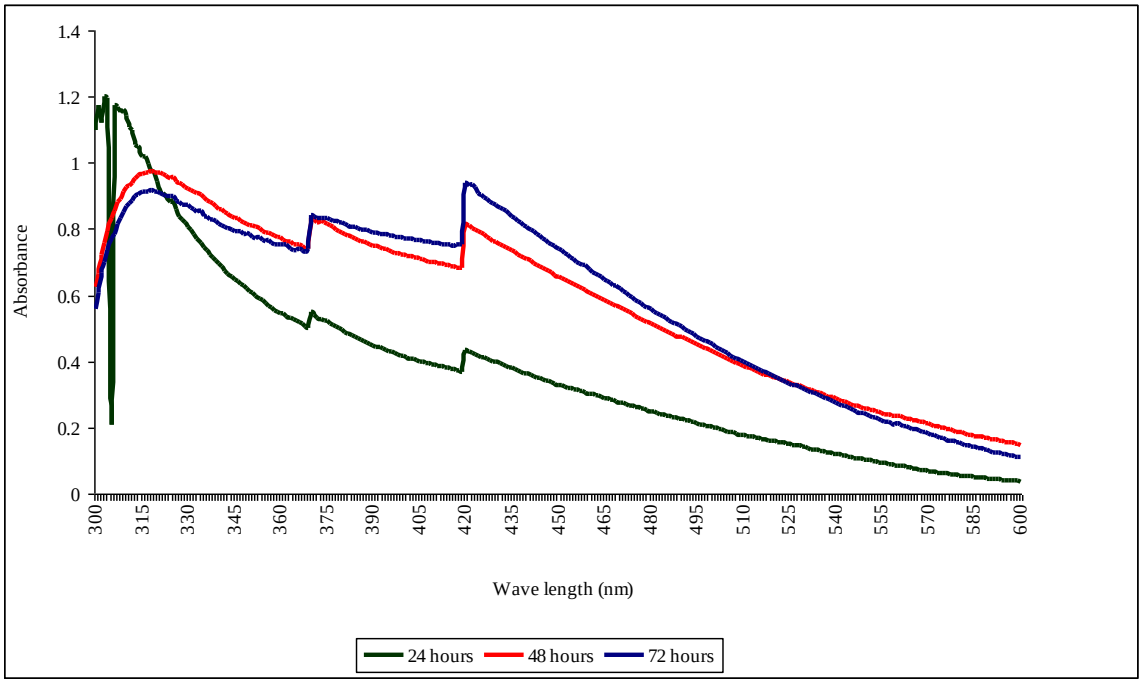

Fig. 3.2 UV- Visible spectra of actinomycete supernatant (+50) filtrate as a function of time. In different incubations with silver nitrate (1mM) after 24h, 48h and 72h. respectively. The peak 420nm corresponds to the plasmon resonance of silver nanoparticles.

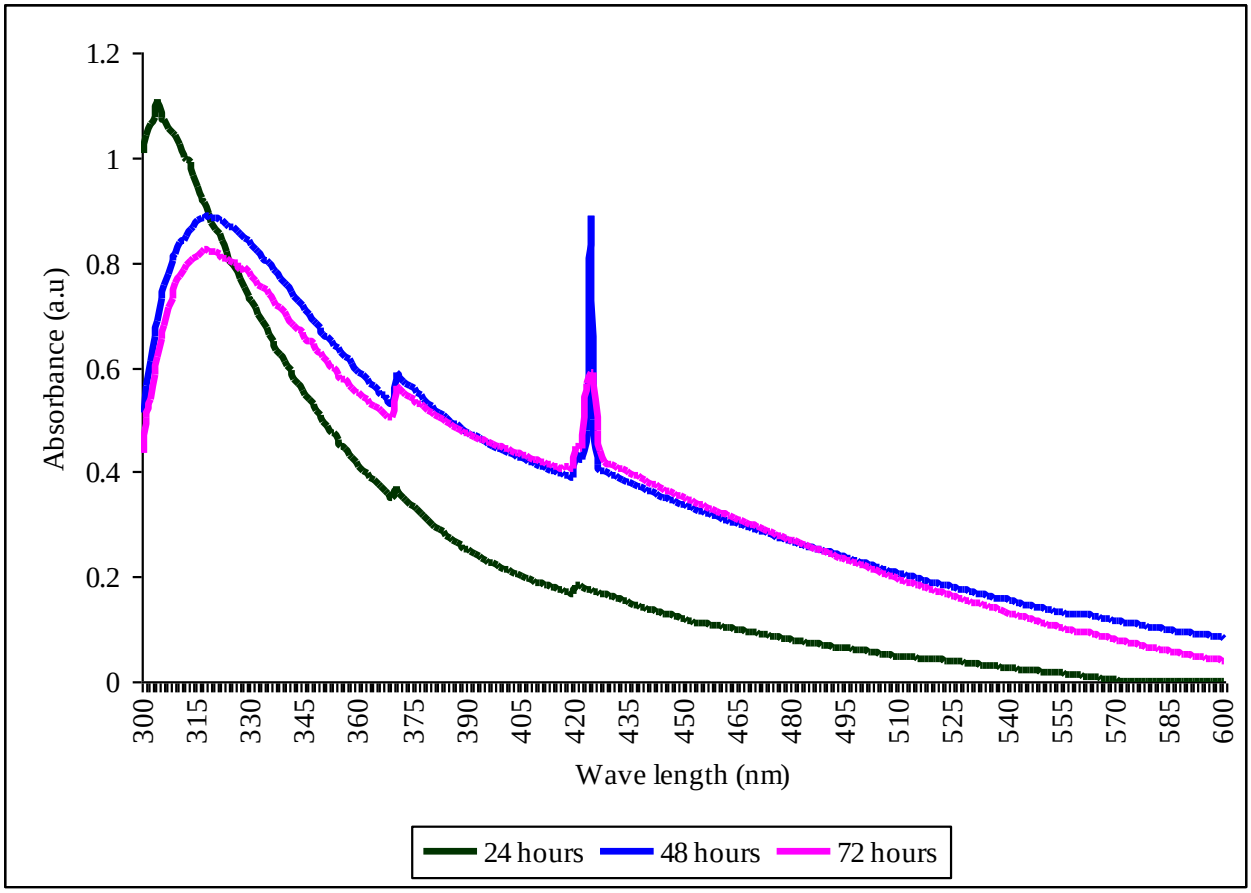

Fig. 3.3 UV- Visible spectra of actinomycete supernatant (+118) filtrate as a function of time. In different incubations with silver nitrate (1mM) after 24h, 48h and 72h. respectively. The peak 420nm corresponds to the plasmon resonance of silver nanoparticles.

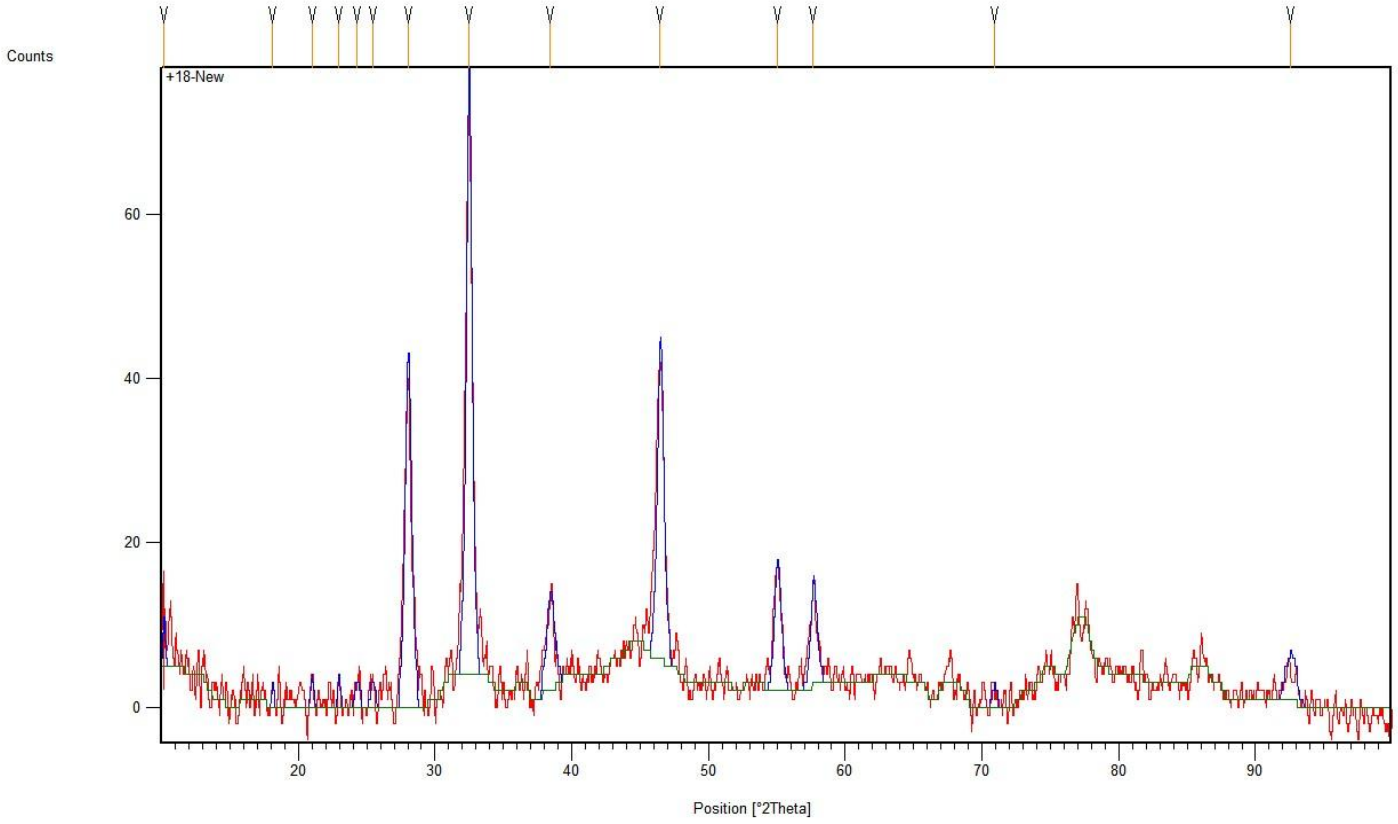

Fig. 3.4 XRD spectra of silver nanoparticles synthesized by +18 actinomycetes

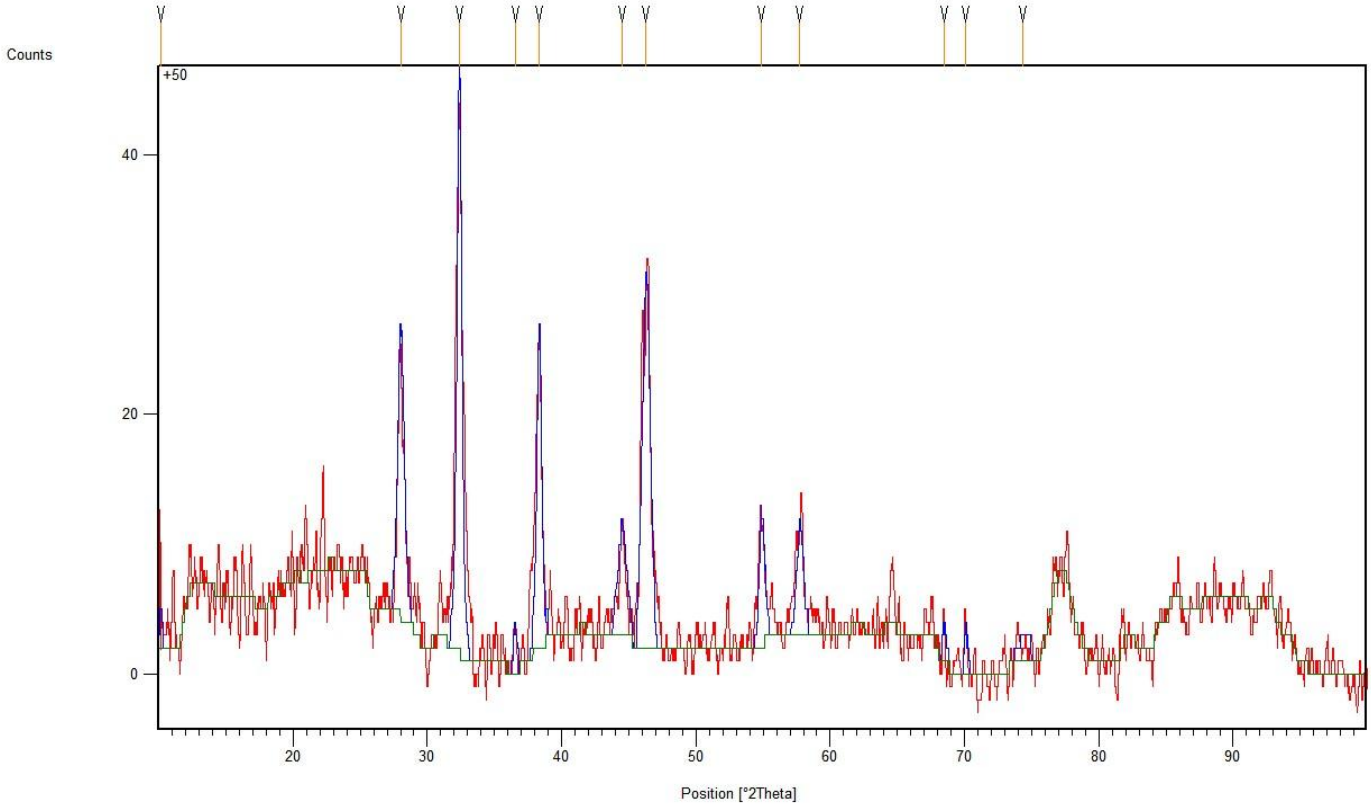

Fig. 3.5 XRD spectra of silver nanoparticles synthesized by +50 actinomycetes

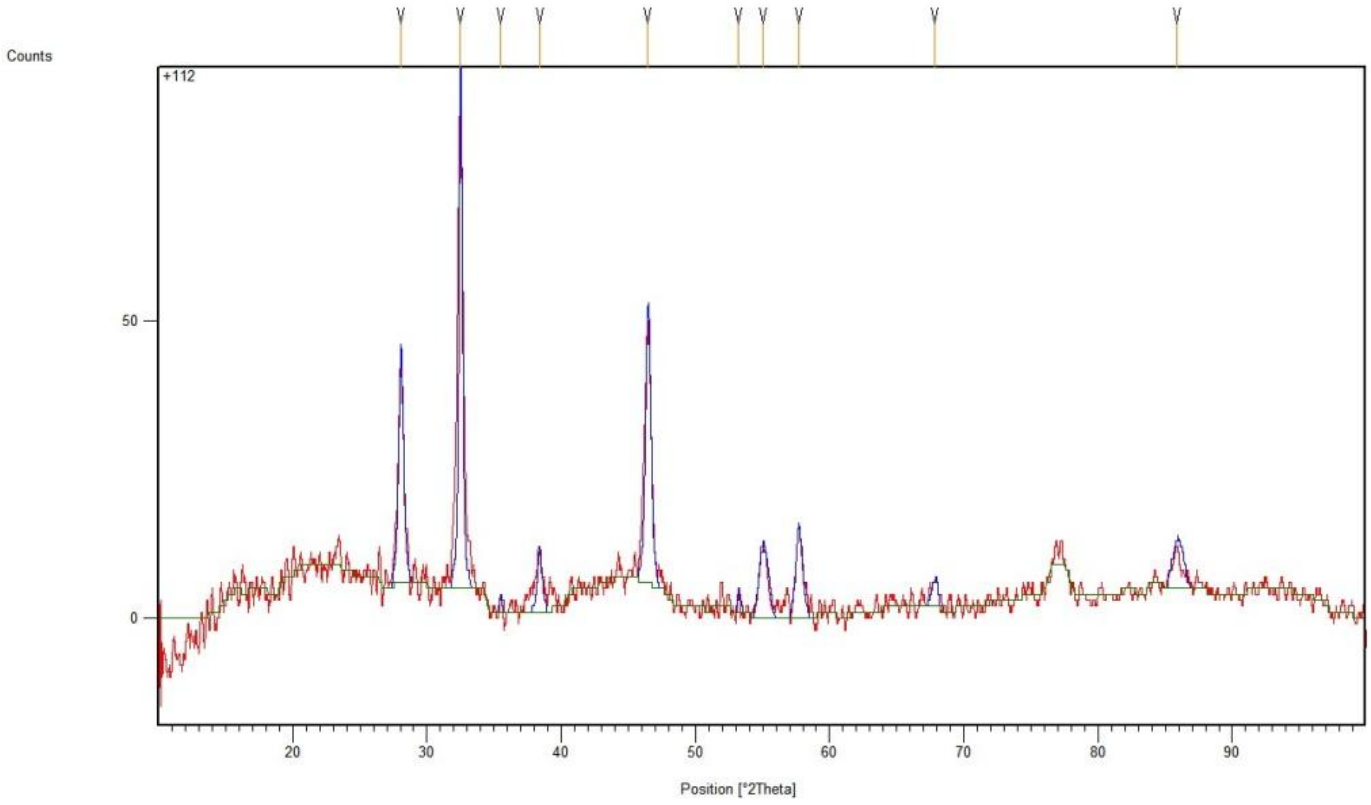

Fig. 3.6 XRD spectra of silver nanoparticles synthesized by +118 actinomycetes

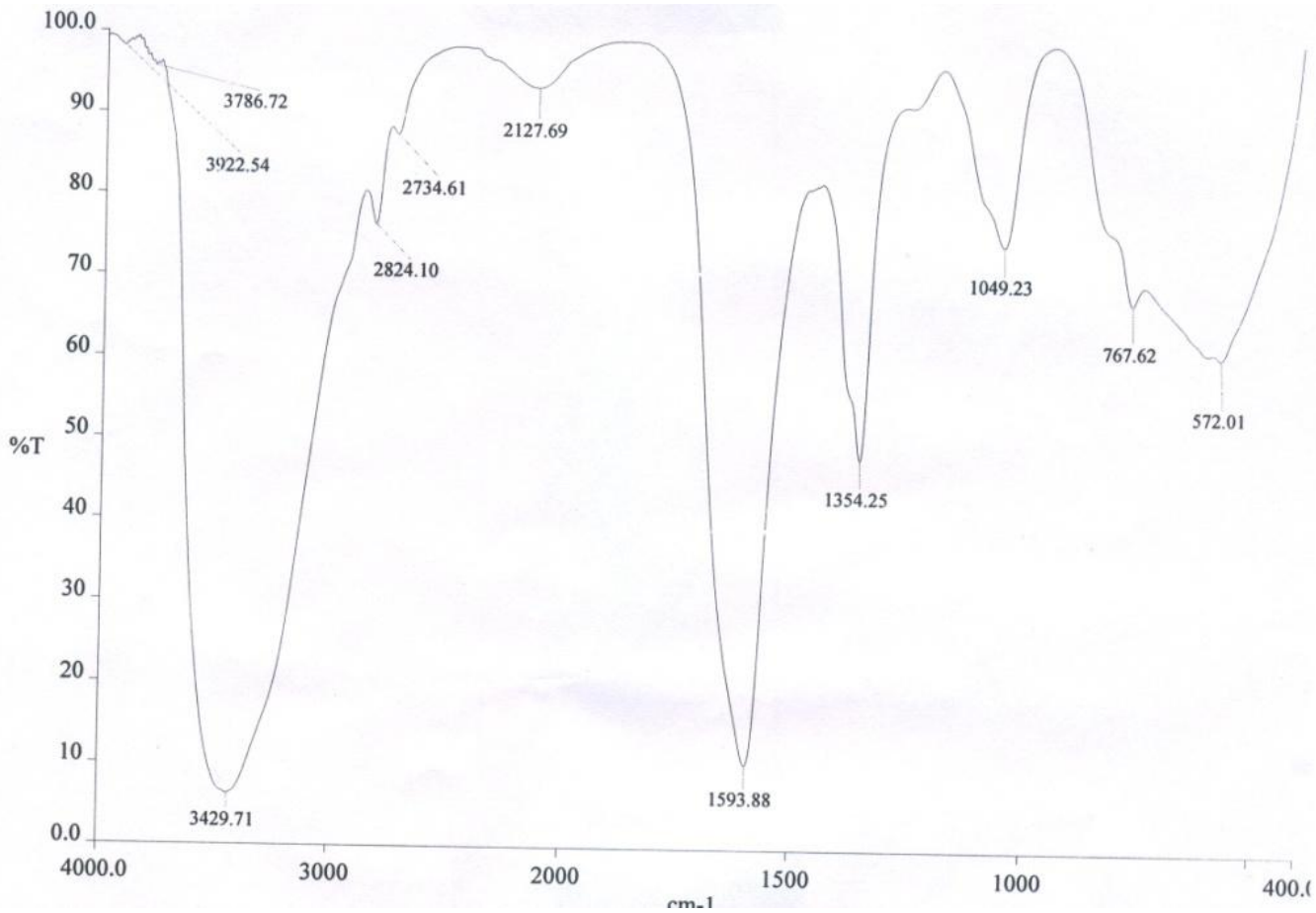

Fig. 3.7 FTIR Spectrum of vaccum dried powder of silver nanoparticles synthesis from 1mM $AgNO_3$ and actinomycete +18 supernatant

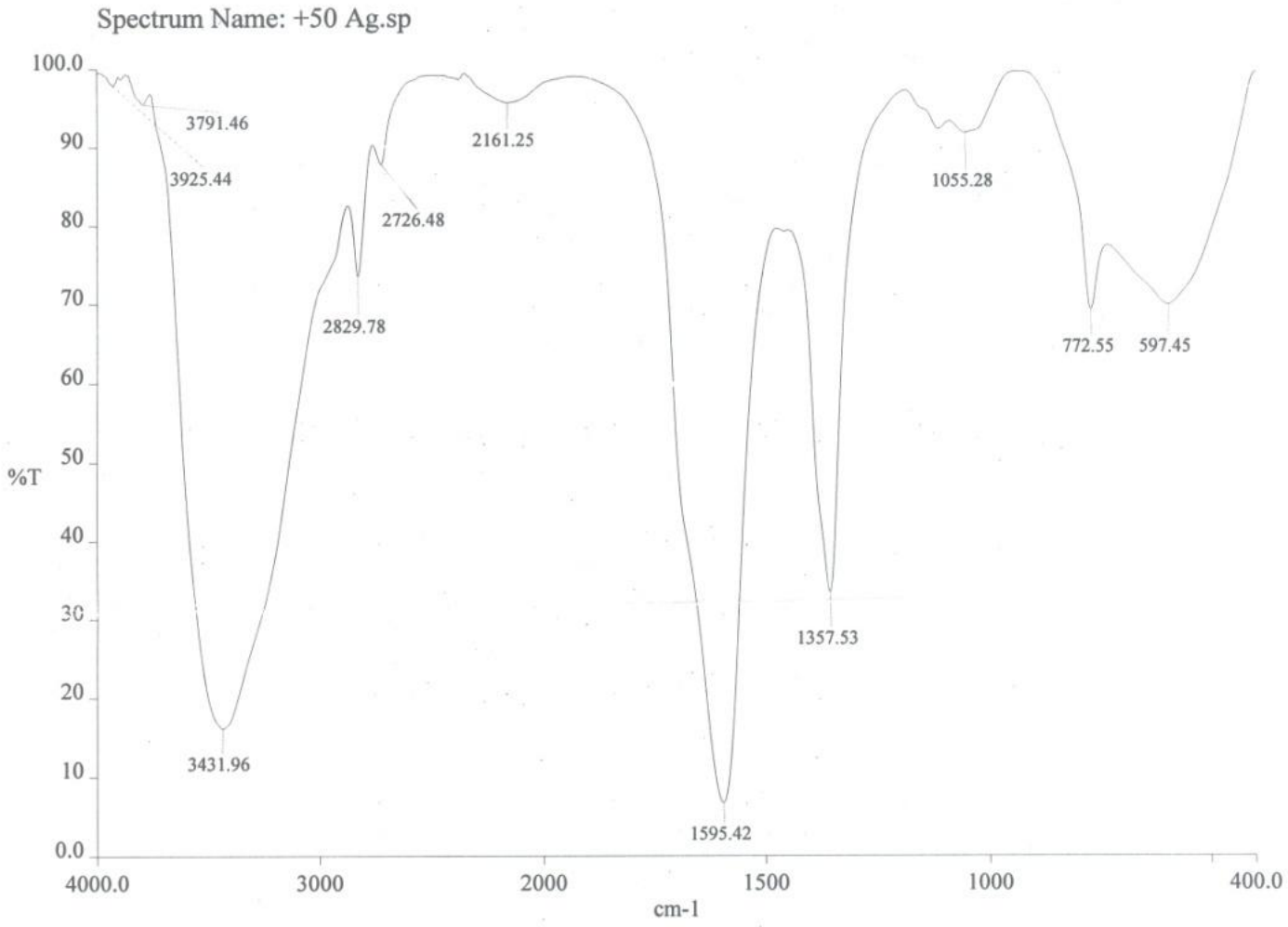

Fig. 3.8 FTIR Spectrum of vaccum dried powder of silver nanoparticles synthesis from 1mM $AgNO_3$ and actinomycete +50 supernatant

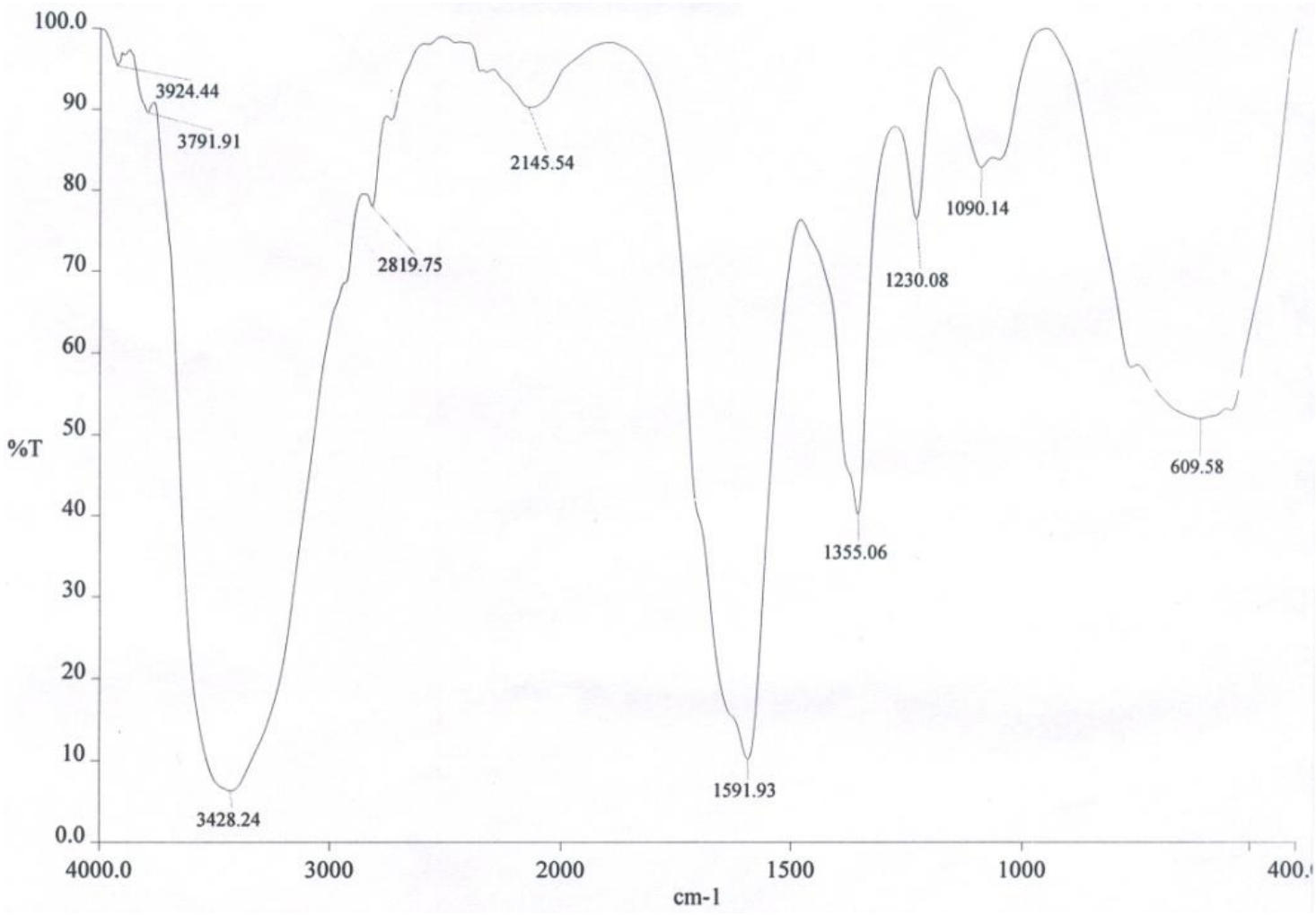

Fig. 3.9 FTIR Spectrum of vaccum dried powder of silver nanoparticles synthesis from 1mM AgNo3 and actinomycete +118 supernatant

Table 5.1 Particle size and structure of silver nanoparticles (X-ray diffraction measurements)

S.No	Strains No	JCPDF file No	2θ peaks	AgNP Size(nm)	Crystalline structure
1	+18	411402	57 (103)	16.89	Primitive Hexagonal
2	+50	893722	38 (111), 44 (200)	20.55,10.65	Cublic face centered
3	+118	87.0598	35(100), 55(006), 67(106)	31.15, 11.15,17.86	Primitive Hexagonal

Table 5.2 Functional groups of AgNPs

S.No	Strains	Total Peaks	Strong Peaks	Functional groups
1	+18	11	3429 1593 1354 1049	OH Stretch Secondary Amine, NH bend Aromatic secondary amine, CN stretch Cyclohexane ring vibrations Methyne (>CH-)
2	+50	11	3433 1595 1357 772	Hydrogen group, H-Bonded OH stretch Primary amine, NH bend Aromatic tertiary amine, CN Stretch Aliphatic chloro compounds. C-CI Stretch
3	+118	10	3428 1591 1355 1230 609	Hydrogen group, H-Bonded OH stretch Primary amine, NH bend Aromatic tertiary amine, CN Stretch Aromatic phosphate P-O-C Stretch Disulfides C-S stretch

Table 5.3 Antimicrobial activity of silver nanoparticles against *E.coli* and *S.aureus*

Actinomycets strain	Zone of inhibition (mm diameter)	
	E.coli	*S.aureus*
+18	5	9
+50	7	8
+118	6	8

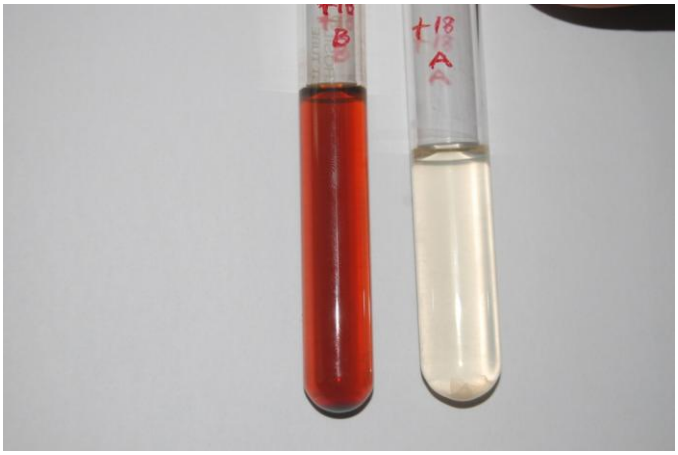

Plate 13 Solution of silver nitrate (1mM) before (A) and after (B) exposure to the culture supernatant of actinomycetes +18

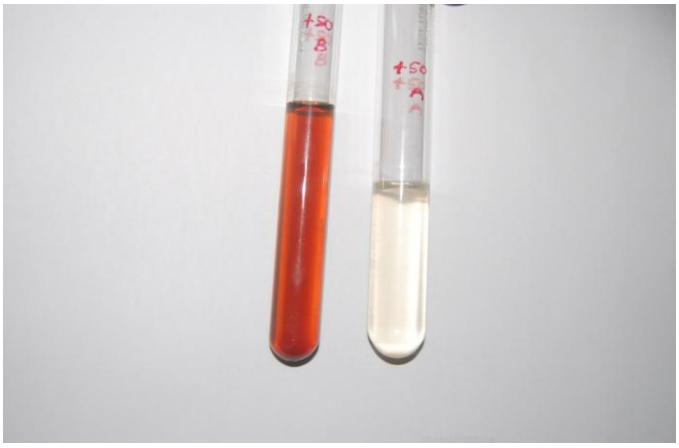

Plate 14 Solution of silver nitrate (1mM) before (A) and after (B) exposure to the culture supernatant of actinomycetes +50

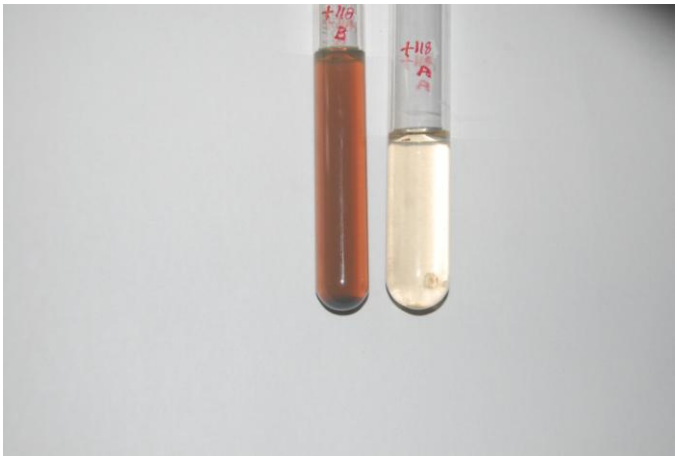

Plate 15 Solution of silver nitrate (1mM) before (A) and after (B) exposure to the culture supernatant of actinomycetes +118

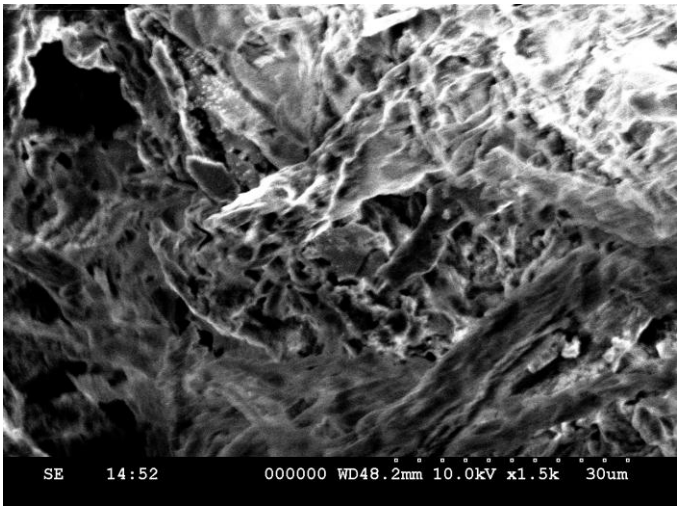

Plate 16 SEM image of silver nanoparticles (+18)

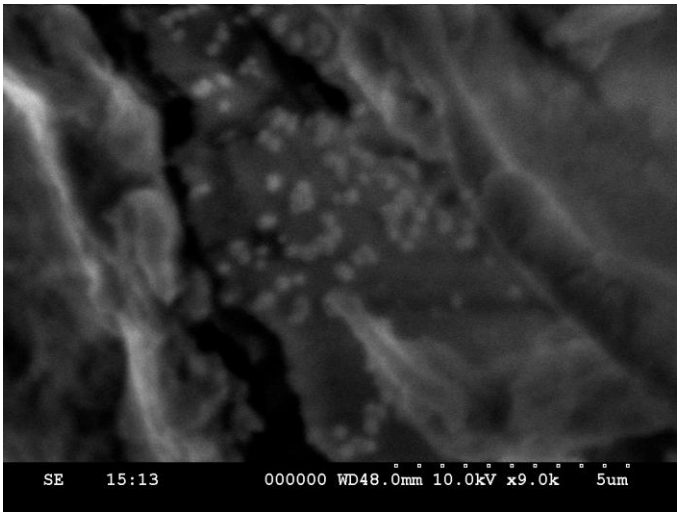

Plate 17 SEM image of silver nanoparticles (+50)

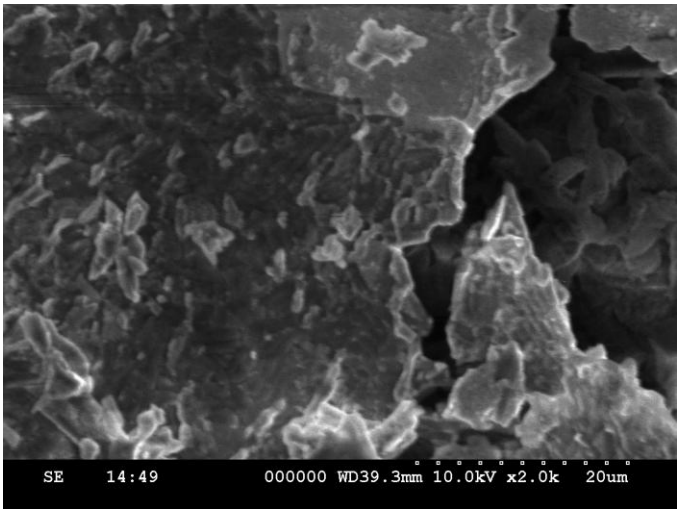

Plate 18 SEM image of silver nanoparticles (+118)

5.4 DISCUSSION

Nanotechnology is a new direction in science and technology, which is intensively developed during the last decade and represents one of the most important directions in the technological developments of the leading countries in 21st century. Today nanotechnologies significantly influence all aspects of our life. Their commercial use involves all branches of industry, medicine, agriculture, etc. Transition from the "micro" to the "nano" represents qualitative rather than quantitative transition form manipulation of the matter to controlled manipulation by individual atoms and molecules. Due to their sizes the nanoparticles acquire new physico-chemical properties and functions, which significantly differ from properties and functions of atoms and molecules constituting large sized particles. *Streptomycetes* have given us a number of useful compounds of various chemical structures, so called as secondary metabolites, including antibiotics (Yoshiko, 2003).

Silver has been known to possess strong antimicrobial properties both in its metallic and nanoparticle forms hence; it has found variety of applications in different fields. The Fe_3O_4 attached Ag nanoparticles can be used for the treatment of water and easily removed using magnetic field to avoid contamination of the environment (Gong *et al.,* 2007). Silver sulfadazine depicts better healing of burn wounds due to its slow and steady reaction with serum and other body fluids (Fox and Modak, 1974). The nanocrystalline silver dressings, creams, gel effectively reduce bacterial infections in chronic wounds (Richard *et al.,* 2002; Leaper, 2006; Ip *et al.,* 2006). The silver nanoparticle containing poly vinyl nano-fibres also show efficient antibacterial property as wound dressing (Jun *et al.,* 2007). The silver nanoparticles are reported to show better wound healing capacity, better cosmetic appearance and scarless healing when tested using an animal model (Tian *et al.,* 2007). Silver impregnated medical devices like surgical masks and implantable devices show significant antimicrobial efficacy (Furno *et al.,* 2004). Environmental-friendly antimicrobial nanopaint can be developed (Kumar *et al.,* 2008). Inorganic composites are used as preservatives in various products (Gupta and Silver, 1998). Silica gel micro-spheres mixed with silica thio-sulfate are used for long

lasting antibacterial activity (Gupta and Silver, 1998). Treatment of burns and various infections (Feng *et al.,* 2000). Silver zeolite is used in food preservation, disinfection and decontamination of products (Matsuura *et al.,* 1997; Nikawa *et al.,* 1997). Silver nanoparticles can be used for water filtration (Jain and Pradeep, 2005).The use of nanoparticulate pharmaceutical carriers to enhance the *in vivo* efficiency of many drugs well established itself over the past decade both in pharmaceutical research and clinical setting. The current level of engineering pharmaceutical nanocarriers in some cases allows for drug delivery systems to demonstrate a combination of some desired properties (Oyewumi and Mumper, 2004).

In this study, the synthesis of silver nanoparticles by using culture supernatant of actinomycetes +18, +50, +118 were investigated. The silver nitrate mediated biosynthesize of AgNPs has passible within 72h of incubation. The appearance of a brown colour in the reaction vessels suggested the formation of silver nanoparticles as reported by the. Ahmed *et al.* (2007 & 2003) who reported that *Klebsiella pneumonia* culture supernatant syntheses silver nanoparticles. Whereas no color change was observed in either the culture supernatant without silver nitrate or the silver nitrate control experiments. The presence of colour may be due to the exciation of surface plasma resonance and the reduction of $AgNo_3$ (Sathasivam *et al.,* 2010).

In the UV spectrum, a strong and broad peak was observed between 420-425nm indicating the presents of AgNPs. It may have occurred due to the reduction of metal ions by secondary metabolites present in the cells. The specific surface plasmon resonance (SPR) future confirmed successful formation of AgNPs. The present study was similar to the earlier findings (Sathasivam *et al.,* 2010; Basavaraja *et al.,* 2008; Asmathunisha Nabikhan, *et al.,* 2010).

Similarly, Parikh *et al.* (2008) reported that, the *Morganella* sp. extracellular syntheses of silver nanoparticles and their size was 20-30nm. Chen *et al.* (2003) reported that, the *Phoma* sp.3.2883 extracellular syntheses of silver nanoparticles and their size

were 71.06 - 74.46nm. *Aspergillus fumigatus* extarcellular syntheses the AgNP and their size was 5-25nm (Bhainsa and D'Souza., 2006).

The SPR patterns and characterization of NPs were found to strongly depend on particle size, stabilizing molecules or surface adsorbed particles as well as the dielectric constant of the medium. A single SPR band in the early stages of synthesis directly corresponded to the absorption spectra of spherical NPs. Many SPR bands were observed when the incubation period was extended and two prominent bands were achieved at 72 and 96 h of incubation, suggesting the formation of anisotropic molecules which were later stabilized in the medium as agreed by (Krishnaraj *et al.,* 2010; Sathasivam *et al.,* 2010).

In the present observation, the characteristic XRD peaks were centered at ~38°, ~45° and ~65°, which could be induced by the following crystalline planes of silver; 111, 200 and 220, respectively. XRD analysis showed the diffraction peaks at which the indexed planes were about 111, 200 and 220 of the cubic face-centered silver. The lattice constant calculated from this pattern was 'a' = 4.086Å and the data obtained matched with the database of the Joint Committee on Powder Diffraction Standards (JCPDS) file No. 04-0783. The average grain size of the AgNPs formed in the bioreduction process was determined using Scherr's formula: $d = (0.9\lambda \times 180°)/\beta\cos\theta\pi$ as opined by earlier workers (Kalishwaralai *et al.,* 2008; Sathasivam *et al.,* 2010).

X-ray diffraction pattern indicated the crystalline structure of silver nanoparticles. The presence of peaks at 2θ values of 35.918, 45.548, 62.688 and 75.758 have been corresponding to (1 1 1), (2 0 0), (2 2 0) and (3 1 1) planes of silver respectively. The XRD spectrum confirmed the presence of silver nanoparticles. The values agree well with those reported for silver (face centric cubic) by Joint Committee on Powder Diffraction Standards File No. 04 - 0783. Similar type of investication was also made earlier by (Kasthuri *et al.,* 2009). Vigneshwaran *et al. (*2007) reported that the scanning electron micrograph of the *Aspergillus flavus* fungal mycelium treated as positive control (incubated with deionized water for 72h.) while fungal mycelium treated with 1.0mM

silver nitrate solution for 72h. The insets show the magnified view of corresponding micrographs. The surface deposited silver nanoparticles are seen clearly at a higher magnification in the silver nitrate treated fungal mycelium.

In our observation, the FTIR was spectrum recorded from the freeze-dried powder of silver nanoparticles formed after 72h of incubation with the fungus. The amide linkages between amino acid residues in proteins increased the well-known signatures in the infrared region of the electromagnetic spectrum. The bands at 3280 cm^{-1} and 2924 cm^{-1} were assigned to the stretching vibrations of primary and secondary amines respectively while their corresponding bending vibrations were seen at 1651 cm^{-1} and 1548 cm^{-1} respectively. The two bands observed at 1379 cm^{-1} and 1033 cm^{-1} can be assigned to the C–N stretching vibrations of aromatic and aliphatic amines respectively. The overall observation was confirmed that the presence of protein in the samples of silver nanoparticles as reported earlier by Gole *et al.* (2001) and Mandal *et al.* (2005) who described the proteins can bind to nanoparticles either through free amine groups or cysteine residues. The binding of protein with silver nanoparticles may plausible due to the electrostatic attraction of negatively charged carboxylate groups in enzymes present in the cell wall of mycelia (Sastry *et al.,* 2003).

Futher, it is also found that the proteins could possibly form a coat covering the metal nanoparticles to prevent their agglomeration and aid in its stabilization in the medium as reported by Balaji *et al.* (2009); Gole *et al.* (2001) and Shaligram *et al.* (2009) who reported that the FTIR Spectroscopic studies on the silver nanoparticles obtained from the fungus, *C.cladosporioides*. Their study confirmed that, the carbonyl group from the amino acid residues and peptides of proteins has strong ability to bind silver. Shrivastava *et al.,* (2007) reported that, the minimum inhibition concentration of extracellular biosynthesized silver nanoparticles on gram negative and gram positive bacteria were determined by broth dilution methods. The observed minimum inhibition concentration values for AgNPs were 30, 35, 80 and 65µg/ml for *E.coli, S.typhi, S.aureus* and *M.luteus* respectively.

In the present study, the silver nanoparticles was showed efficient antimicrobial property compared to other salts due to their extremely large surface area, which provides better contact with microorganisms. The nanoparticles get attached to the cell membrane and also penetrate inside the bacteria. The bacterial membrane contains sulfur-containing proteins and the silver nanoparticles interact with these proteins in the cell as well as with the phosphorus containing compounds like DNA. When the silver nanoparticles enter into the bacterial cell it forms a low molecular weight region in the center of the bacteria to which the bacteria conglomerates thus, protecting the DNA from the silver ions. The nanoparticles preferably attack the respiratory chain, cell division finally leading to cell death. The nanoparticles release silver ions in the bacterial cells, which enhance their bactericidal activity (Feng *et al*., 2000; Sondi and Salopek-Sondi, 2007; Morones *et al*., 2005; Song *et al*., 2006). Several workers reported high antimicrobial activity of silver nanoparticles against various pathogens.

Nanda and Saravanan (2009) reported that, the synthesis of silver nanoparticles from the *Staphylococcus aureus* and the antimicrobial activity of silver nanoparticles were investigated against various pathogenic organisms such as MRSA, MRSE, *S.pyogens, S.typhi, K.pneumoniae* and *V.cholarae* using well diffusion methods. The highest antimicrobial activity was observed against MRSA followed by MRSE and *S.pyogenes*. The minimum activity was found against *S.typhi* and *K.pneumoniae*, but against *V.cholerae* no zone of inhibition was recored. Sondi and Salopeak-Sondi (2004) used *E.coli* as a model for gram negative bacteria and proved that AgNPs as an antimicrobial agent. Shahverdi *et al.* (2007) have reported that the AgNPs have an antimicrobial effect on *S.aureus* and *E.coli.*

The surface plasmon resonance plays a major role in the determination of optical absorption spectra of metal nanoparticles, which shifts to a longer wavelength with increase in particle size. The size of the nanoparticle implies that it has a large surface area to come in contact with the bacterial cells and hence, it will have a higher percentage of interaction than bigger particles so that in the present study even a small contant of silver nanoparticles can inhibit the bacterial growth very effectively (Kreibig and

Vollmer, 1995; Mulvaney, 1996; Morones *et al.,* 2005; Pal *et al.,* 2007). The nanoparticles smaller than 10nm interact with bacteria and produce electronic effects, which enhance the reactivity of nanoparticles. Thus, it is corroborated that the bactericidal effect of silver nanoparticles is size dependent as reported by Raimondi *et al.* (2005) and Morones *et al.* (2005). The antimicrobial efficacy of the nanoparticle also depended on the shapes of the nanoparticles as reported by Morones *et al.* (2005). According to Pal *et al.* (2007) truncated triangular nanoparticles showed bacterial inhibition with silver content of 1μg. While, in case of spherical nanoparticles total silver content of 12.5μg is needed. The rod shaped particles needed a total of 50 to 100μg of silver content. Thus, the silver nanoparticles with different shapes have different effects on bacterial cell.

Bharde *et al.* (2005) have demonstrated that magnetite nanoparticle synthesis by *Actinobacter*, a non magnetotactic bacterium. In prior studies, the biosynthesis of magnetite was found to be extremely slow (often requiring 1 week) under strictly anaerobic conditions. However, this study reported that the *Actinobacter* sp. were capable of magnetite synthesis by reaction with suitable aqueous iron precursors under fully aerobic conditions. Importantly, the extracellular magnetite nanoparticles showed excellent magnetic properties.